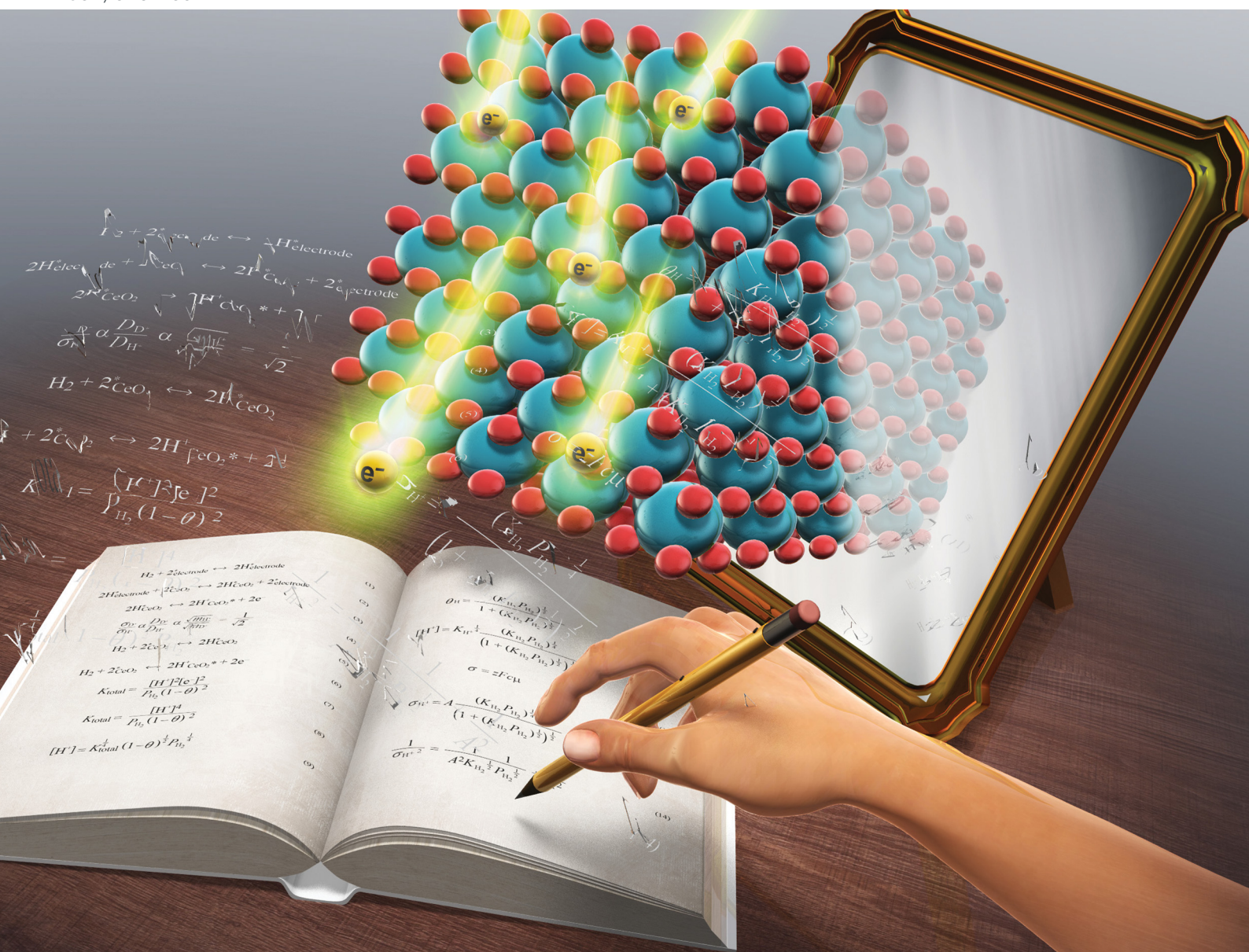


ChemComm

Chemical Communications

rsc.li/chemcomm



ISSN 1359-7345




Cite this: *Chem. Commun.*, 2022, 58, 10789

Received 3rd July 2022,
Accepted 2nd September 2022

DOI: 10.1039/d2cc03687h

rsc.li/chemcomm

Quantitative investigation of CeO₂ surface proton conduction in H₂ atmosphere†

Taku Matsuda, Ryo Ishibashi, Yoshiki Koshizuka, Hideaki Tsuneki and
Yasushi Sekine *

This report is the first describing a study quantitatively analysing aspects of oxide surface protonics in a dry H₂ atmosphere. Elucidating surface protonics is important for electrochemical and catalytic applications. In this study, AC impedance spectroscopy was used to investigate surface conduction properties of porous CeO₂ at low temperatures (423–573 K) and in a dry H₂ atmosphere. Results demonstrated that the conductivity increased by several orders of magnitude when H₂ was supplied. Dissociative adsorption of H₂ contributes to conduction by forming proton–electron pairs. Also, H/D isotope exchange studies confirmed protons as the dominant conduction carriers. Furthermore, H₂ adsorption equilibrium modelling based on the Langmuir mechanism was applied to explain the H₂ partial pressure dependence of conductivity. For the first time, the obtained model explains the experimentally obtained results both qualitatively and quantitatively. These findings represent new insights into surface protonics in H₂ atmosphere.

The phenomenon of surface protonics has potential applications in proton-conducting fuel cells,¹ proton exchange membranes² and electrochemical gas sensors.³ This phenomenon is defined as proton transfer at oxide surfaces. Moreover, surface protonics plays an important role in heterogeneous catalysis.^{4–17} Surface proton conduction is observed in the presence of H₂O or H₂ at temperatures of room temperature to 773 K.^{18–31} Because adsorption plays an important role, porous samples at low temperatures are preferred; for H₂O adsorption, multilayers are formed. It is noteworthy that no multilayer is formed in the adsorption of H₂, thereby leading to a difference in surface proton transport behaviour: in an H₂O atmosphere, free protons and mainly hydronium ions move through the chemisorbed and physisorbed water layers on the oxide, respectively according to the Grotthuss and vehicle mechanisms.²⁹ Which mechanism prevails depends on the water layer thickness in relation to temperature and

relative humidity.²⁹ However, in an H₂ atmosphere, dissociative adsorption of H₂ produces proton–electron pairs. The produced protons are transferred on the surface lattice oxygen by a hopping mechanism.³¹ The presence of a metal (e.g. Pt) is regarded as necessary for H₂ dissociation and spillover.

The evaluation of surface proton conduction is of great importance. For that evaluation, AC impedance spectroscopy is a promising technique because it allows separation of the electrical properties into components (e.g. bulk and grain boundaries), and facilitates their subsequent quantified. To date, many reports have described studies using AC impedance measurements to characterise surface proton conduction properties in an H₂O atmosphere.^{18–30} Earlier reports described that surface proton conductivity under an H₂O atmosphere can be quantified using an equivalent circuit suitable for the analysis.^{28–30} The equivalent circuit included surface components parallel to the bulk and grain boundary components, thereby allowing direct assessment of surface proton transport in the adsorbed water layer.

However, the evaluation of surface proton conduction under a dry H₂ atmosphere has been reported only qualitatively.³¹ It has not yet reached the stage of quantitative evaluation. Therefore, a more general theory of surface proton conduction under a dry H₂ atmosphere must be found.

This study investigated surface proton conduction properties induced by dry H₂ supply on porous CeO₂ by AC impedance measurements. Then a model was proposed to interpret those properties in terms of H₂ partial pressure dependence. This study provides new insights into surface proton conduction in H₂ atmosphere on an oxide surface. As the sample to be measured, we selected CeO₂ (JRC-CEO-1), because surface protonic transport on CeO₂ has been widely studied^{25–28} and CeO₂ as a surface proton-conducting oxide is important for catalysis and fuel cell applications.^{4–12,27} Experimental procedures are described in ESI.†

First, the H₂ supply effects on conductivity for porous CeO₂ were investigated at various temperatures by AC impedance measurement. The obtained data were analysed using a parallel

Department of Applied Chemistry, Waseda University, 3-4-1, Okubo, Shinjuku, Tokyo, 169-8555, Japan. E-mail: ysekine@waseda.jp

† Electronic supplementary information (ESI) available. See DOI: <https://doi.org/10.1039/d2cc03687h>



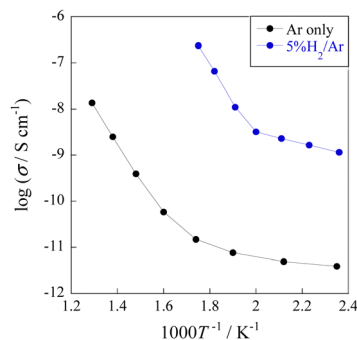
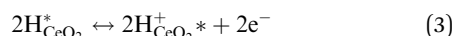


Fig. 1 Temperature dependence of conductivity for CeO₂ under Ar and 5%H₂/Ar atmospheres.

RQ equivalent circuit presented in Fig. S1 (ESI[†]). The temperature dependence of the CeO₂ conductivity with and without H₂ supply is presented in Fig. 1. From these data, we inferred that the H₂ supply increased the conductivity by several orders of magnitude. The marked increase in conductivity is not attributable to oxygen vacancy formation, as explained in the discussion of ESI[†] (see Fig. S2 and S3). A change in the activation energy was also observed before and after H₂ supply, as shown in Table 1, suggesting a change in the conduction mechanism or conductive carriers. According to earlier reports, porous samples with relative density of around 60% provide information related to conduction with adsorbed species.^{28,31} As shown in Fig. S4 in ESI[†], SEM observations confirmed the presence of numerous pores in samples with relative density of approximately 60%.

The increase in conductivity can therefore be attributed to the dissociative adsorption of H₂ and the formation of conducting species, as presented in eqn (1)–(3).



Therein, * denotes adsorption site. Hydrogen spillover has been reported earlier.^{32,33}

Dissociative adsorption of H₂ is thought to have occurred on the Pt electrode. It then spilled over onto CeO₂, giving rise to proton and electron pairs. On various reducible oxides (*e.g.* CeO₂, TiO₂, WO₃), protons are said to bind to surface lattice oxygen; electrons reduce metal cations near O–H bonds.³⁴ Protons move over the oxide surface, whereas electrons move *via* the conduction band.

Table 1 Apparent activation energy of conduction for each condition

Condition (—)	Activation energy (eV)
Ar only (> 573 K)	1.33
Ar only (< 573 K)	0.18
5%H ₂ /Ar (> 500 K)	1.48
5%H ₂ /Ar (< 500 K)	0.24

Table 2 H/D isotope effects on conductivity at each temperature

Temp (K)	$\sigma_{\text{D}}/\sigma_{\text{H}}$ (—)
573	0.79
548	0.67
523	0.59
498	0.72
473	0.69
448	0.68
423	0.69

Next, the H/D isotope effect was investigated to identify the dominant conducting carrier in the H₂ atmosphere. As a result, the H/D isotope effect was identified at each measured temperature, as shown in Table 2 and in Fig. S5 in ESI[†]. Those findings are explainable by the different barriers posed by the hopping mechanism against the transfer of protons and deuterons. The deuteron transfer barrier is well known to be higher than the proton transfer barrier because of the different energies of the O–H and O–D ground states. According to classical theory, the theoretical value of the H/D isotope effect on the hopping proton/deuteron conductivity $\sigma_{\text{D}}/\sigma_{\text{H}}$ is expected to be $\frac{1}{\sqrt{2}}$ (≈ 0.71),^{35,36} as calculated using the following equation.³⁷

$$\frac{\sigma_{\text{D}^+}}{\sigma_{\text{H}^+}} \propto \frac{D_{\text{D}^+}}{D_{\text{H}^+}} \propto \frac{\sqrt{m_{\text{H}^+}}}{\sqrt{m_{\text{D}^+}}} = \frac{1}{\sqrt{2}} \quad (4)$$

In that equation, *D* denotes diffusivity; *m* stands for the mass of the diffusing species. As Table 2 shows, the theoretical value closely approximates the experimentally obtained values. It can therefore be inferred that protons are the dominant conduction carrier in the H₂ atmosphere and that they are transferred *via* the hopping mechanism. The possibility of proton conduction in the bulk was ruled out; in general, the diffusivity of hydrogen in CeO₂ is low,³⁸ and considerably high temperatures (above 1050 K) are required for CeO₂ to exhibit the bulk proton conduction.³⁹ So we attributed the measured proton conductivity only to the oxide surface and not to the bulk.

Next, to elucidate the surface protonics in an H₂ atmosphere further, the effects of the H₂ partial pressure dependence were investigated. As Fig. 2 shows, the conductivity increased

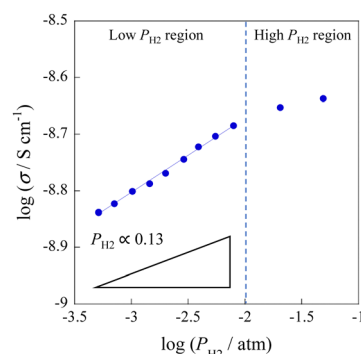
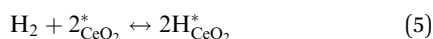


Fig. 2 H₂ partial pressure dependence of conductivity for CeO₂ at 473 K.

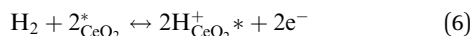


concomitantly with increasing H₂ partial pressure. At the low H₂ partial pressure region, the slope was 0.13. It then saturated gradually with increasing H₂ partial pressure, indicating a relation between conductivity and H₂ coverage. Based on these results, an H₂ adsorption equilibrium model was proposed to interpret the H₂ partial pressure dependence of conductivity.

As explained in the preceding section, dissociative adsorption of H₂ and spillover lead to the formation of protons on the CeO₂ surface, as shown particularly by eqn (1)–(3). For simplicity, eqn (1) and (2) were combined. The reaction on the Pt electrode was omitted.



The total equation for eqn (3) and (5) and the equilibrium constant K_{total} can be written as



$$K_{\text{total}} = \frac{[\text{H}^+]^2 [\text{e}^-]^2}{P_{\text{H}_2} (1 - \theta)^2} \quad (7)$$

where θ denotes the coverage over CeO₂. Considering charge neutrality ($[\text{H}^+] = [\text{e}^-]$), the following equation is obtainable.

$$K_{\text{total}} = \frac{[\text{H}^+]^4}{P_{\text{H}_2} (1 - \theta)^2} \quad (8)$$

Then, rearranging eqn (8) yields the following equation.

$$[\text{H}^+] = K_{\text{total}}^{\frac{1}{4}} (1 - \theta)^{\frac{1}{2}} P_{\text{H}_2}^{\frac{1}{4}} \quad (9)$$

This equation represents the H₂ partial pressure dependence of proton concentration. However, the relation between H₂ partial pressure and coverage is not considered. The H₂ partial pressure dependence is explainable by the Langmuir adsorption model. The Langmuir adsorption model includes the assumption that the adsorption sites are homogeneous without interactions and that no interaction exists between neighbouring adsorbed molecules. The model also describes the adsorption of molecules on a solid surface as a function of gas pressure at a constant temperature. Applying the Langmuir adsorption model to eqn (5) gives the following equation.

$$\theta_{\text{H}} = \frac{(K_{\text{H}_2} P_{\text{H}_2})^{\frac{1}{2}}}{1 + (K_{\text{H}_2} P_{\text{H}_2})^{\frac{1}{2}}} \quad (10)$$

Therein, K_{H_2} denotes the Langmuir adsorption constant. The H₂ atom coverage represented in the eqn (10) can be assumed to be similar to θ . Then, substituting the coverage in the eqn (9) yields the following equation.

$$[\text{H}^+] = K_{\text{H}^+}^{\frac{1}{4}} \frac{(K_{\text{H}_2} P_{\text{H}_2})^{\frac{1}{4}}}{\left(1 + (K_{\text{H}_2} P_{\text{H}_2})^{\frac{1}{2}}\right)^{\frac{1}{2}}} \quad (11)$$

In that equation, K_{H^+} is the equilibrium constant for eqn (5). The carrier concentration such as that of protons is related to the conductivity.

$$\sigma = zFc\mu \quad (12)$$

Therein, z , F , c , and μ respectively denote the charge number, Faraday's constant, carrier concentration, and mobility.

Substituting the proton concentration expressed in eqn (11) into eqn (12) yields the following equation.

$$\sigma_{\text{H}^+} = A \frac{(K_{\text{H}_2} P_{\text{H}_2})^{\frac{1}{4}}}{\left(1 + (K_{\text{H}_2} P_{\text{H}_2})^{\frac{1}{2}}\right)^{\frac{1}{2}}} \quad (13)$$

In this equation, $A = F\mu_{\text{H}^+} K_{\text{H}^+}^{\frac{1}{4}}$

Therefore, the following can be inferred from eqn (13); (1) At low H₂ partial pressures, $(K_{\text{H}_2} P_{\text{H}_2})^{\frac{1}{2}} \ll 1$. Then the proton conductivity is proportional to the power of 1/4 of the H₂ pressure. (2) At high H₂ partial pressures, $(K_{\text{H}_2} P_{\text{H}_2})^{\frac{1}{2}} \gg 1$. Then the proton conductivity is independent of the H₂ partial pressure. These conclusions show close agreement with the experimentally obtained results. Furthermore, to explain the dependence of conductivity on H₂ partial pressure quantitatively rather than qualitatively, eqn (13) can be rearranged as shown below.

$$\frac{1}{\sigma_{\text{H}^+}^2} = \frac{1}{A^2 K_{\text{H}_2}^{\frac{1}{2}} P_{\text{H}_2}^{\frac{1}{2}}} + \frac{1}{A^2} \quad (14)$$

The values of A and K_{H_2} are obtainable by the slope and intercept of $\frac{1}{\sigma_{\text{H}^+}^2}$ vs. $\frac{1}{P_{\text{H}_2}^{\frac{1}{2}}}$. The relation between $\frac{1}{\sigma_{\text{H}^+}^2}$ vs. $\frac{1}{P_{\text{H}_2}^{\frac{1}{2}}}$ is shown in Fig. 3.

As expected, a linear relation was confirmed. The values of A and K_{H_2} were calculated respectively as $2.5 \times 10^{-9} \text{ S cm}^{-1}$ and $4.8 \times 10^2 \text{ atm}^{-1}$. Substituting these values in the eqn (13) enables calculation of the value of σ_{H^+} at the H₂ partial pressure. A comparison of the experimentally obtained data with the calculated data is presented in Fig. 4. The calculated σ_{H^+} showed good correspondence with the experimentally obtained results, thereby proving the model validity.

In summary, AC impedance measurements were taken to characterise the electrical properties of porous CeO₂ in a dry H₂ atmosphere. A marked increase in conductivity with H₂ supply was observed, suggesting the formation of conductive carriers

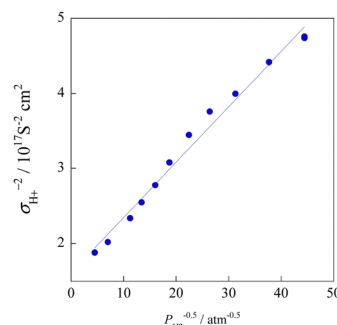


Fig. 3 Relation between $P_{\text{H}_2}^{-0.5}$ and $\sigma_{\text{H}^+}^{-2}$.



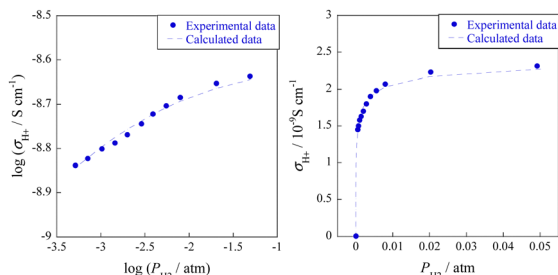


Fig. 4 H_2 partial pressure dependence of conductivity for CeO_2 at 473 K: experimentally obtained data and calculated data.

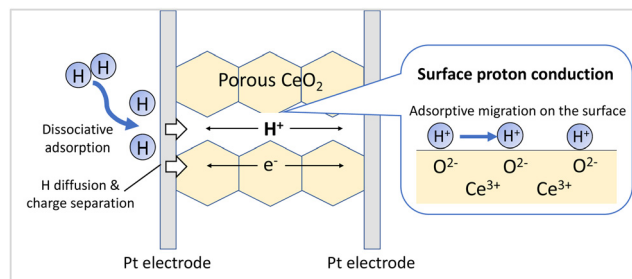


Fig. 5 Schematic image of the surface proton conduction in a dry H_2 condition on CeO_2 .

(protons and electrons) by dissociative adsorption of H_2 as shown in Fig. 5. The H/D isotope effect was also observed, indicating protons as the dominant conductive carriers. Furthermore, the proposed H_2 adsorption equilibrium model quantitatively describes the H_2 partial pressure dependence of the conductivity. The model presented herein provides new insights into surface protonics in a dry H_2 atmosphere. The development of surface protonics in a dry H_2 atmosphere and the establishment of a method for measuring and evaluating such protonics are expected to be applied to various catalytic reactions such as ammonia synthesis in a dry H_2 atmosphere in the future.

Conflicts of interest

The authors have no conflicts of interest.

References

- 1 S. Kim, H. Park, M. Martin and Z. Munir, *Adv. Mater.*, 2008, **20**, 556–559.
- 2 A. Shabanikia, M. Javanbakht, H. Salar Amoli, K. Hooshyari and M. Enhessari, *J. Electrochem. Soc.*, 2014, **161**, 1403–1408.
- 3 M. Sakthivel and W. Weppner, *J. Phys. D: Appl. Phys.*, 2007, **40**, 7210–7216.
- 4 M. Torimoto, S. Ogo, Y. Hisai, N. Nakano, A. Takahashi, Q. Ma, J. G. Seo, H. Tsuneki, T. Norby and Y. Sekine, *RSC Adv.*, 2020, **10**, 26418–26424.
- 5 A. Takahashi, R. Inagaki, M. Torimoto, Y. Hisai, T. Matsuda, Q. Ma, J. G. Seo, T. Higo, H. Tsuneki, S. Ogo, T. Norby and Y. Sekine, *RSC Adv.*, 2020, **10**, 14487–14492.
- 6 K. Murakami, Y. Tanaka, R. Sakai, Y. Hisai, S. Hayashi, Y. Mizutani, T. Higo, S. Ogo, J. G. Seo, H. Tsuneki and Y. Sekine, *Chem. Commun.*, 2020, **56**, 3365–3368.
- 7 K. Yamada, S. Ogo, R. Yamano, T. Higo and Y. Sekine, *Chem. Lett.*, 2020, **49**(3), 303–306.
- 8 K. Takise, A. Sato, S. Ogo, J. G. Seo, K. Imagawa, S. Kado and Y. Sekine, *RSC Adv.*, 2019, **9**, 27743–27748.
- 9 M. Torimoto, K. Murakami and Y. Sekine, *Bull. Chem. Soc. Jpn.*, 2019, **92**(10), 1785–1792.
- 10 K. Takise, A. Sato, K. Murakami, S. Ogo, J. G. Seo, K. Imagawa, S. Kado and Y. Sekine, *RSC Adv.*, 2019, **9**, 5918–5924.
- 11 R. Inagaki, R. Manabe, Y. Hisai, Y. Kamite, T. Yabe, S. Ogo and Y. Sekine, *Int. J. Hydrogen Energy*, 2018, **43**(31), 14310–14318.
- 12 R. Manabe, S. Okada, R. Inagaki, K. Oshima, S. Ogo and Y. Sekine, *Sci. Rep.*, 2016, **6**, 38007.
- 13 M. Kosaka, T. Higo, S. Ogo, J. G. Seo, K. Imagawa, S. Kado and Y. Sekine, *Int. J. Hydrogen Energy*, 2020, **45**(1), 738–743.
- 14 T. Yabe, K. Yamada, K. Murakami, K. Toko, K. Ito, T. Higo, S. Ogo and Y. Sekine, *ACS Sustainable Chem. Eng.*, 2019, **7**(6), 5690–5697.
- 15 A. Gondo, R. Manabe, R. Sakai, K. Murakami, T. Yabe, S. Ogo, M. Ikeda, H. Tsuneki and Y. Sekine, *Catal. Lett.*, 2018, **148**(7), 1929–1938.
- 16 K. Murakami, R. Manabe, H. Nakatsubo, T. Yabe, S. Ogo and Y. Sekine, *Catal. Today*, 2018, **303**, 271–275.
- 17 R. Manabe, H. Nakatsubo, A. Gondo, K. Murakami, S. Ogo, H. Tsuneki, M. Ikeda, A. Ishikawa, H. Nakai and Y. Sekine, *Chem. Sci.*, 2017, **8**, 5434–5439.
- 18 S. Kim, H. J. Avila-Paredes, S. Wang, C. T. Chen, R. A. Souza, M. Martin and Z. A. Munir, *Phys. Chem. Chem. Phys.*, 2009, **11**, 3035–3038.
- 19 B. Scherrer, M. V. F. Schlupp, D. Stender, J. Martynczuk, J. G. Grolig, H. Ma, P. Kocher, T. Lippert, M. Prestat and L. J. Gauckler, *Adv. Funct. Mater.*, 2013, **23**, 1957–1964.
- 20 M. T. Colomer, *Adv. Mater.*, 2006, **18**, 371–374.
- 21 H. J. Avila-Paredes, J. Zhao, S. Wang, M. Pietrowski, R. A. de Souza, A. Reinholdt, Z. A. Munir, M. Martin and S. Kim, *J. Mater. Chem.*, 2010, **20**, 990–994.
- 22 S. Miyoshi, Y. Akao, N. Kuwata, J. Kawamura, Y. Oyama, T. Yagi and S. Yamaguchi, *Solid State Ionics*, 2012, **207**, 21–28.
- 23 S. Miyoshi, Y. Akao, N. Kuwata, J. Kawamura, Y. Oyama, T. Yagi and S. Yamaguchi, *Chem. Mater.*, 2014, **26**, 5194–5200.
- 24 R. Sato, S. Ohkuma, Y. Shibuta, F. Shimajo and S. Yamaguchi, *J. Phys. Chem. C*, 2015, **119**, 28925–28933.
- 25 G. Gregori, M. Shirpour and J. Maier, *Adv. Funct. Mater.*, 2013, **23**, 5861–5867.
- 26 M. Shirpour, G. Gregori, R. Merkle and J. Maier, *Phys. Chem. Chem. Phys.*, 2011, **13**, 937–940.
- 27 Y. Xing, Y. Wu, L. Li, Q. Shi, J. Shi and S. Yun, *ACS Energy Lett.*, 2019, **4**, 2601–2607.
- 28 R. Manabe, S. Ø. Stub, T. Norby and Y. Sekine, *Solid State Commun.*, 2018, **270**, 45–49.
- 29 S. Ø. Stub, E. Vøllestad and T. Norby, *J. Phys. Chem. C*, 2017, **121**, 12817–12825.
- 30 S. Ø. Stub, E. Vøllestad and T. Norby, *J. Mater. Chem. A*, 2018, **6**, 8265–8270.
- 31 Y. Hisai, K. Murakami, Y. Kamite, Q. Ma, E. Vøllestad, R. Manabe, T. Matsuda, S. Ogo, T. Norby and Y. Sekine, *Chem. Commun.*, 2020, **56**, 2699–2702.
- 32 K. Mori, N. Hashimoto, N. Kamiuchi, H. Yoshida, H. Kobayashi and H. Yamashita, *Nat. Commun.*, 2021, **12**, 3884.
- 33 F. Yang, B. Hu, W. Xia, B. Peng, J. Shen and M. Muhler, *J. Catal.*, 2018, **365**, 55–62.
- 34 W. C. Conner and J. L. Falconer, *Chem. Rev.*, 1995, **95**, 759–788.
- 35 J. Bigeleisen, *J. Chem. Phys.*, 1949, **17**, 675–678.
- 36 T. Scherban, W. K. Lee and A. S. Nowick, *Solid State Ionics*, 1988, **28–30**, 585–588.
- 37 T. Scherban, Y. Baikov and E. Shalkova, *Solid State Ionics*, 1993, **66**, 159–164.
- 38 N. Sakai, K. Yamaji, T. Horita, H. Yokokawa, Y. Hirata, S. Sameshima, Y. Nigara and J. Mizusaki, *Solid State Ionics*, 1999, **125**, 325–331.
- 39 Y. Nigara, K. Kawamura, T. Kawada, J. Mizusaki and M. Ishigame, *J. Electrochem. Soc.*, 1999, **146**, 2948–2953.

